

## Variability of apparent diffusion coefficients in metastatic small cell lung carcinoma: comparisons between-within normal tissue and liver metastases

Ernesto Roldán-Valadez,\* David Cortez-Conradis,\* Alejandro Ríos-Hoyo,\*\* Óscar Arrieta\*\*\*

\* Magnetic Resonance Unit, Medica Sur Clinic & Foundation. Mexico City, Mexico.

\*\* Division of Health Sciences, Anahuac University. Mexico City, Mexico.

\*\*\* Thoracic Oncology Clinic, National Cancer Institute of Mexico and Medica Sur Clinic & Foundation, Mexico City.

### ABSTRACT

In recent years, the use of diffusion weighted MRI (DW-MRI) has increased for the diagnosis of focal liver lesions (FLLs). DW-MRI may help in the differentiation of benign and malignant FLLs by measuring the apparent diffusion coefficient (ADC) values. Unfortunately, liver metastases present different histopathologic features with variable MRI signals within each lesion; this histologic variability explains the intra- and inter-lesion variations of ADC measurements. We present the case of a 64-year-old female with diagnosis of liver metastasis from small cell lung carcinoma admitted to the emergency unit due to symptoms of inappropriate antidiuretic hormone secretion. Quantitative comparison of two liver MRI, on admission and 2-months after transcatheter arterial chemoembolization showed persistence of the hyperintense metastatic lesions with significant difference in the ADC values in the with-in metastatic lesions ( $p = 0.001$ ) and between normal tissue and liver metastases only at the end of treatment ( $p < 0.001$ ). Several publications state that DW-MRI is capable to predict the response to chemotherapy in malignant tumors, the histologic variability of liver metastasis and their response to different treatments is reflected in intra- and inter-lesion variations of ADC measurements that might delay an accurate imaging diagnosis. We present evidence of this variability, which might encourage prospective clinical trials that would define better cut-off values, would help understand the ADC biological behaviour, and would reach consensus about the best acquisition parameters for this promising quantitative biomarker.

**Key words.** Diffusion magnetic resonance imaging. Liver. Neoplasm metastasis. Small cell lung carcinoma. Therapeutic chemoembolization.

### INTRODUCTION

The liver is the most common site for metastatic tumor deposits with evidence of hepatic metastases reported in 36% of all patients who died from cancer.<sup>1</sup> A diffuse infiltration to the liver can lead to fulminant hepatic failure, this entity is defined as liver disease that causes encephalopathy within 8 weeks of onset of symptoms in a patient with no prior evidence of liver disease.<sup>2</sup>

Among the causes of secondary infiltration of the liver, hematologic malignancies are the most common cause;<sup>1</sup> small cell lung carcinoma is a highly-invasive primary tumor, its hepatic metastases are common, however their presentation as acute hepatic failure resulting from diffuse parenchymal infiltration is rare.<sup>3</sup>

Magnetic resonance imaging (MRI) provides an excellent tissue contrast, greater than any other imaging modality; since more a decade, MRI has proved to be markedly superior to computed tomography (CT) in the detection and characterization of focal liver lesions (FLLs), with these differences having clinical significance.<sup>4</sup> Regarding safety, this method is a safer modality than CT, both the imaging system itself and the intravenous contrast agent employed.<sup>5,6</sup>

The unenhanced and dynamic (post contrast) images in liver MRI are considered conventional

---

Correspondence and reprint request: Ernesto Roldán-Valadez, M.D., M.Sc. Magnetic Resonance Unit, Medica Sur Clinic & Foundation  
Puente de Piedra 150, Toriello Guerra. C.P. 14050, Mexico City, Mexico.  
Tel.: +5255 5666-1625  
E-mail: ernest.roldan@usa.net

*Manuscript received: May 23, 2013.  
Manuscript accepted: December 12, 2013.*

sequences, in recent years, quantitative sequences such as diffusion weighted MRI (DW-MRI) has been increasingly used for the diagnosis of FLLs. DW-MRI can improve detection and differentiation of benign and malignant FLLs both by means of visual assessment and calculation of apparent diffusion coefficient (ADC) values.<sup>7</sup> It can help direct the attention of the radiologist and clinicians to imaging findings that may otherwise be overlooked; a combination of DWI and conventional MRI has been proved to increase the diagnostic performance of this technique in the characterization of benign and malignant liver lesions.<sup>8</sup>

In this report we present the MRI findings and quantitative evaluation of DWI measures in a patient with liver metastases from small lung cell carcinoma, as well as a brief review of the basic concepts of DWI and its clinical applications in liver imaging.

### CASE REPORT

A 64-year-old female started her current disease 24 months before this report with symptoms of dry cough; a chest X-ray and CT-scan demonstrated a right perihilar lung nodule. She underwent thoracoscopy-guided biopsy with a punch biopsy; histolo-

gical findings of the nodule specimen documented undifferentiated small cell lung carcinoma. After the diagnostic work-up, multimodality therapeutic approach was chosen consisting of induction chemotherapy (etoposide and cisplatin for 4 months) followed by thoracic concurrent chemo-radiotherapy; a brain MRI showed no evidence of metastatic disease. Five months after the initial diagnosis, the syndrome of inappropriate antidiuretic hormone secretion (SIADH) was diagnosed and the patient received a second line chemotherapy with irinotecan and carboplatin. Two months later, she developed malignant pleural effusion and underwent thoracoscopy with removal of 1,500 cm<sup>3</sup> of pleural and 250 cm<sup>3</sup> of pericardial fluid. During the year before the admission for this report, a massive pleural effusion developed again and liver metastasis were detected and treated with selective transarterial chemoembolization (TACE) of the left hepatic artery using irinotecan.

On day 1st of this report, the patient was admitted to the emergency unit for a new episode of hyponatremia, she underwent a whole-body PET-CT which detected multiple hepatic lesions, a right pleural effusion, and an increase in the cerebellar metabolism. Additional diagnostic work-up included a liver MRI to characterize the liver

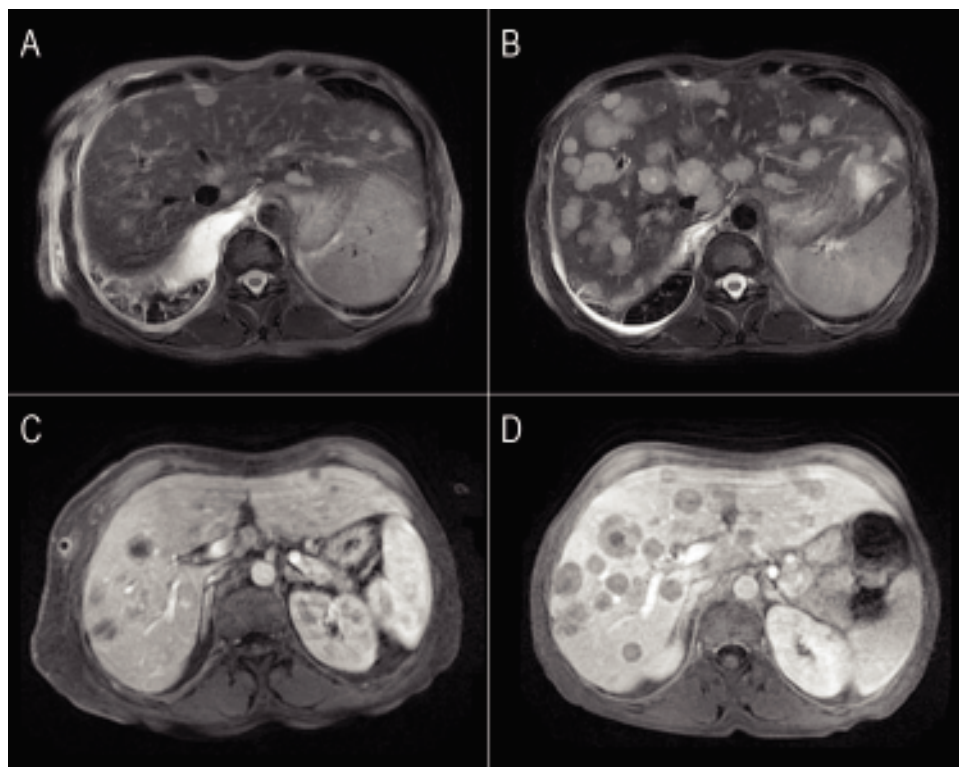


**Figure 1.** Conventional MRI images of liver metastases from small lung cell carcinoma. A, B. Fat-suppressed T2-weighted fast spin-echo images. C, D. Gadolinium-enhanced hepatic arterial dominant-phase 3-dimensional gradient-echo. Multiple areas of distinctly hyperintensity suggesting the possibility of metastases are seen on T2-weighted image (A-B) and on gadolinium-enhanced images (C-D). Notice the increase in number and size for most lesions in the 2-months follow-up (B-D).

lesions; the patient underwent TACE of the right hepatic artery using doxorubicin and a follow-up liver-MRI was scheduled two months after.

The comparison, of the two MRI evaluations revealed multiple areas of distinctly hyperintensity on the conventional MRI sequences, T2-weighted and gadolinium-enhanced images; there was an increase in the number and size of lesions in the follow-up MRI (Figure 1). The diffusion weighted (DW) images also showed multiple areas of hyperintensity from metastatic lesions (Figures 2A and 2B). The quantitative evaluation using ADC maps after DW-MRI data post processing, allowed the inclusion of regions of interest (ROIs) drawn just within the outer border of selected metastasis (we chose lesions measuring more than 2 cm in its maximum axial diameter) and also over an adjacent areas of normal liver parenchyma on the  $b = 500 \text{ s/mm}^2$  images (Figures

2C and 2D). For both kinds of tissues (metastases and normal liver), ADC values showed a normal distribution, which allowed the performance of parametric tests.

An independent-samples t-test was conducted to compare the ADC values for normal tissue and liver metastasis for each evaluation time (admission and follow-up). There was a significant difference between tissues only in the 2-months evaluation:  $t(26) = 5.228$ ,  $p < 0.001$  (two-tailed). The magnitude of the differences in the means (mean difference = 0.000466, 95% CI: 0.000283 to 0.000649) showed a large effect-size (eta squared = 0.498). The changes in ADC values along the follow-up period, reflecting the biological variability of the lesions were evaluated using a paired-samples t-test, separated for each kind of tissue: normal liver and metastasis. There was a statistically significant decrease in ADC

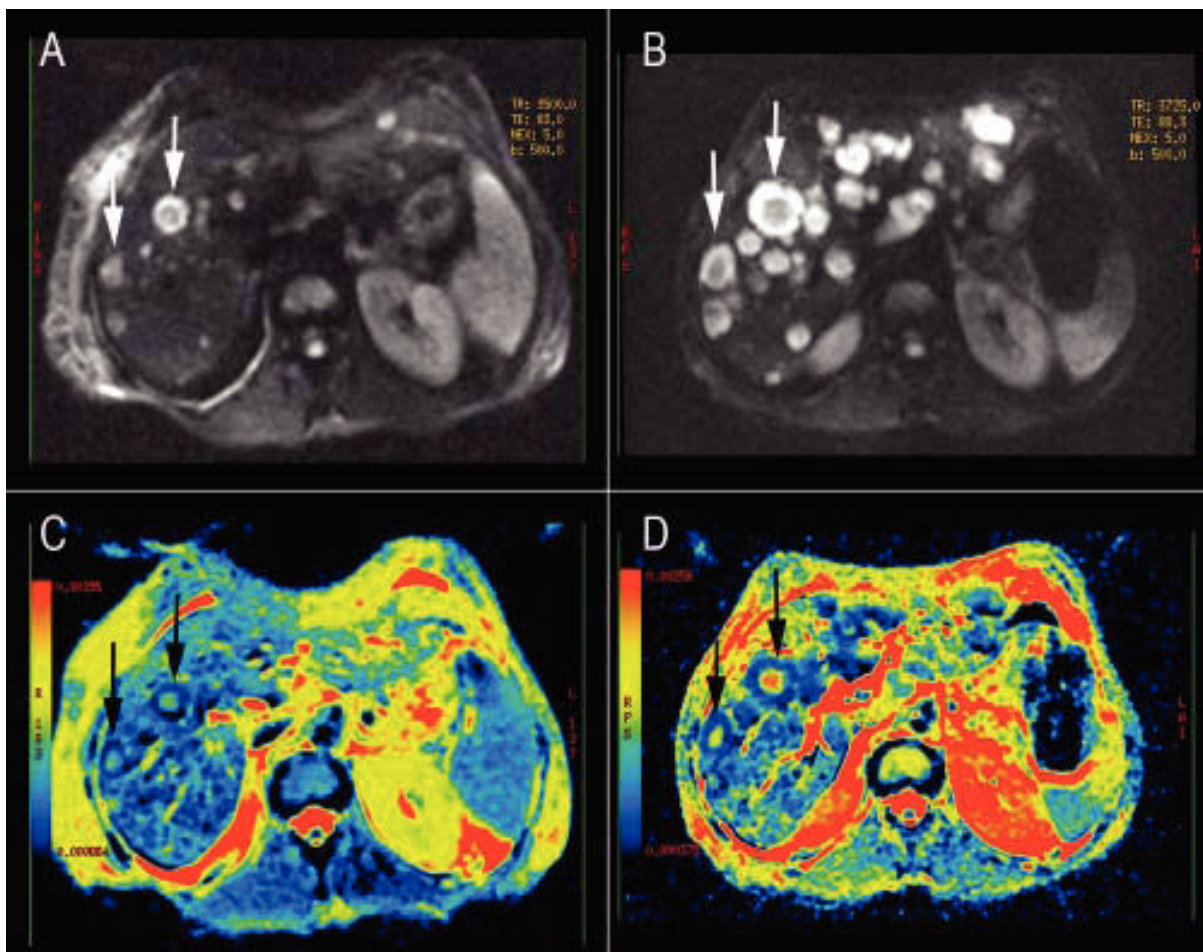


**Figure 2.** Diffusion weighted (DW) images of the liver in a patient with metastatic small cell lung cancer. A, B. DW images ( $b$  value,  $500 \text{ s/mm}^2$ ) showing multiple areas of hyperintensity from metastatic lesions. C, D. ADC maps of the correspondent DW images; it is possible to identify the variability in the intensity-dependent colouring of some metastatic lesions, showing a darker cell-dense rim and a colored necrotic center (white arrows). B-D DWI image and ADC map from the follow-up evaluation.

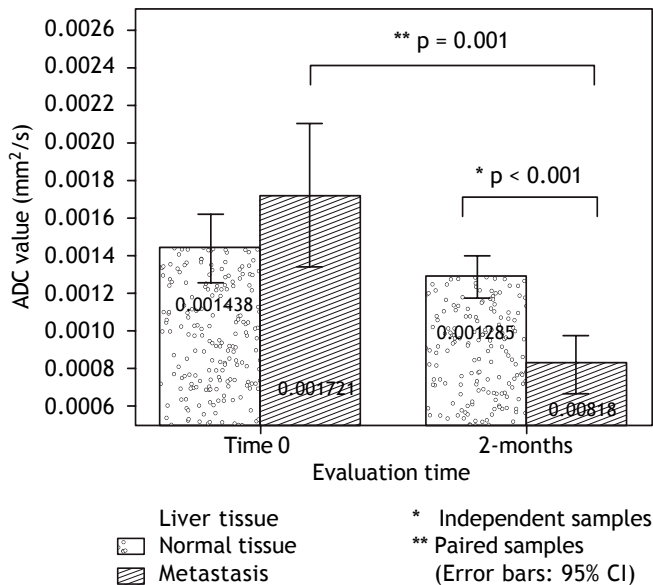


**Figure 3.** Bar graphs depicting the significant variability observed between-tissues (normal tissue vs. metastasis) and within lesions (metastatic tissue) in the ADC measurements after a 2-month follow-up evaluation. Normal distribution of data allowed the performance of parametric tests.

values from the admission to 2-months follow-up:  $t(9) = 4.676$ ,  $p = 0.001$  (two-tailed). The mean decrease in ADC values (0.000849 with a 95% confidence interval ranging from 0.000438 to 0.001260) also showed a large effect size (eta-squared = 0.548). Labels of the mean ADC values are observed on bar graphs of figure 3. The patient received medication for the SIADH symptoms and continued her treatment in the medical oncology outpatient clinic.

## DISCUSSION

The initial clinical application of DW-MRI for visualizing the restriction of water molecule diffusion was in the hyperacute diagnosis of brain infarction in 1986,<sup>9</sup> Nowadays, DW-MRI is part of routine MR imaging protocols for detecting and characterizing FLLs, and has served as supplementary sequence for  $T_1$ -/ $T_2$ - weighted and gadolinium-enhanced MR imaging.<sup>10</sup> Promising data has been reported for the detection and differentiation of benign and malignant lesions, staging of lesions for oncology patients, as well as follow-up treatments for liver tumors.<sup>11</sup> It is thought that DW-MRI is capable of predicting the response to chemotherapy of malignant tumors.<sup>12</sup>

What clinicians should understand about DW-MRI is that, it is represented by the ADC value (in  $\text{mm}^2/\text{s}$ ), which detects random motion of water mo-

lecules and overall cellular integrity and, thus, can be used to distinguish viable cells from dead tumor cells by revealing differences in membrane permeability.<sup>13</sup> Cellular necrosis causes increased membrane permeability, which allows water molecules to move freely, thereby causing a relative increase in the ADC value; water movement of intracellular, extracellular and vascular molecules also influence ADC measurements.<sup>14</sup>

Low ADC values will depict a restricted or impeded diffusion in tissues with high cellularity, e.g. tumors, abscesses, fibrosis and cytotoxic edema; on the other hand, high ADC values represent a relative free or unimpeded diffusion which is encountered in tissues with low cellularity or tissues with disrupted cell membranes, for example in cysts and necrotic tissue.<sup>15</sup>

The imaging diagnosis of liver metastases is commonly based on follow-up imaging and findings of interval progression (in size and number) and typical enhancement characteristics of liver lesions in conventional MRI images;<sup>16</sup> unfortunately, although ADC measurements efficiently discriminate hepatic cysts, from hepatocellular carcinoma (HCC), liver metastasis and cavernous hemangioma; ADC values tend to decrease in the order of hemangiomas, HCCs, and metastases, with such a substantial overlap of values that makes differentiation virtually impossible;<sup>17</sup> this histologic variability might influence intra- and inter-lesion variations in ADC measurements.

In many cases, hepatic metastases depict peripheral hyperintense rims thought to represent live cancer cells surrounding central dark signals that might represent a combination of fibrosis and coagulation necrosis.<sup>18,19</sup> Metastatic lesions from colorectal, breast, and lung primary tumors, often present with a ring-like pattern on ADC maps, exhibiting low ADC values in the periphery (mean value  $0.001050 \text{ mm}^2/\text{s}$ ) and high ADC values in the center, thought to correspond to central necrosis (mean value  $0.001430 \text{ mm}^2/\text{s}$ ), these findings were observed in our patient (Figure 2).<sup>20</sup> Also, benign hepatic lesions generally exhibit higher ADC values compared with malignant lesions, and various ADC cut-off values ( $0.001400$ - $0.001600 \text{ mm}^2/\text{s}$ ) have been suggested in the literature for the differentiation of benign and malignant FLLs.<sup>20</sup>

To the best of our knowledge, there have not been reports about the diagnostic accuracy of ADC in small-cell lung cancer metastasis, although it is expected to be not too much different from the diagnostic accuracy for colorectal liver metastasis,

estimated at 0.83-0.90,<sup>21</sup> with sensitivity and specificity of 0.82 and 0.94, respectively.<sup>13</sup>

Clinicians should be aware that in the ADC analysis of liver lesions, the sensitivity of the ADC measurements depends on a supplementary parameter of the DW-MRI named the b-value, it summarizes the influence of the gradients during the ADC measurements; the higher the b-value, the more sensitive the sequence is to diffusion effects.<sup>14</sup> Additional technical factors, can all influence estimates of ADC values.<sup>22</sup>

Due to the variability in the ADC measures, even ADC values of lesions of the same histologic type may show overlap and there is no consensus about the best cutoff values for ADC measures in normal parenchyma, benign and malignant lesions. In our patient, we do not have explanation for the non-significant decrease in the post-embolization ADC values observed in normal tissue, current reports on treatment response of liver lesions focused only on changes observed in tumor lesions; we hypothesized that the observed values reflect a normal variability of the liver pushed to the lower side by the TACE treatment, as it disrupts and cuts off the blood supply, resulting in tumor necrosis identified by absence of contrast enhancement after treatment.<sup>23</sup> We believed the decreased blood supply could have an effect in the surrounding normal tissue, by decreasing the global water content, this might lower the ADC values in normal tissue compared with its pre-embolization stage. There was an evident overlap between normal tissue and metastasis in the first ADC comparison, which was not significant. In the literature, the reported mean ADC value of metastases range between 0.000940-0.001500 mm<sup>2</sup>/s; this range is mainly due because every study group uses their own MRI scanning parameters. The combined evaluation of conventional sequences and quantitative analysis of ADC values, has improved the detection of FLLs compared to malignant lesions with sensitivity and specificity values reported in range between 74-100%.<sup>20</sup> The sensitivity of MRI in detection of the liver tumor smaller than 2 cm has been calculated around 33%.<sup>24</sup>

Despite the need for an uniformly applicable scanning protocol to eliminate discrepancies in ADC values caused by different scanning parameters,<sup>17</sup> and the overlap between ADC values of benign and malignant FLL reported in various series in the literature,<sup>7</sup> some positive reports should be mentioned: besides the conventional evaluation of tumor response to chemotherapy and radiation therapy by measuring the percentage of reduction in tumor size after chemotherapy; recent studies using DW-MRI

showed that high pre-treatment ADC values in colorectal liver metastases are predictive of a poor response to oxaliplatin and 5-fluorouracil-based chemotherapy;<sup>25</sup> non-responding tumors and liver parenchyma have not showed significant changes in ADC values.<sup>26</sup> On the other hand, responding tumors have showed a significant increase in ADC values at the end of the treatment,<sup>25</sup> which suggests a change from a more cellular pre-treatment stage to a less cellular or necrotic phenotype.<sup>14</sup>

In our case, the ADC values were not helpful to discriminate between normal liver and metastatic lesions in the baseline evaluation, however it depicted significant differences in the follow-up that would allow stratifying lesions as responders and nonresponders. The decrease in ADC values after the treatment reflected the non-responsive histology of the tumor (undifferentiated small cell lung carcinoma). Similar studies using a b-value of 500, observed mean ADC values in the range of 0.000990-0.001040 mm<sup>2</sup>/s  $\pm$  0.24 (SD) for liver metastasis;<sup>27-29</sup> and ADC values less than 0.000900 mm<sup>2</sup>/s may reflect the possibility of poorly differentiated HCC to post-therapeutic tumor recurrence and poor prognosis.<sup>30</sup>

In conclusion, although the current imaging parameters of DW-MRI still depict a great overlap between ADC values of benign and malignant lesions; there is a promising value of this biomarker in the assessment of tumor response and in the stratification of patients as responders and nonresponders. Future clinical trials including ADC maps of patients with different histologic types of FLLs will help define the diagnostic accuracy of this MRI modality.

## REFERENCES

1. Rowbotham D, Wendon J, Williams R. Acute liver failure secondary to hepatic infiltration: a single centre experience of 18 cases. *Gut* 1998; 576-80.
2. Bernuau J, Rueff B, Benhamou JP. Fulminant and subfulminant liver failure: definitions and causes. *Semin Liver Dis* 1986; 97-106. Doi: 10.1055/s-2008-1040593.
3. Miyaaki H, Ichikawa T, Taura N, Yamashima M, Arai H, Obata Y, Furusu A, et al. Diffuse liver metastasis of small cell lung cancer causing marked hepatomegaly and fulminant hepatic failure. *Intern Med* 2010; 1383-6.
4. Semelka RC, Martin DR, Balci C, Lance T. Focal liver lesions: comparison of dual-phase CT and multisequence multiplanar MR imaging including dynamic gadolinium enhancement. *J Magn Reson Imaging* 2001; 397-401.
5. Reid A, Smith FW, Hutchison JM. Nuclear magnetic resonance imaging and its safety implications: follow-up of 181 patients. *Br J Radiol* 1982; 784-6.
6. Terens WL, Gluck R, Golimbu M, Rofsky NM. Use of gadolinium-DTPA-enhanced MRI to characterize renal mass in patient with renal insufficiency. *Urology* 1992; 152-4.

7. Parikh T, Drew SJ, Lee VS, Wong S, Hecht EM, Babb JS, Taouli B. Focal liver lesion detection and characterization with diffusion-weighted MR imaging: comparison with standard breath-hold T2-weighted imaging. *Radiology* 2008; 812-22. Doi: 10.1148/radiol.2463070432.
8. Naganawa S, Kawai H, Fukatsu H, Sakurai Y, Aoki I, Miura S, Mimura T, et al. Diffusion-weighted imaging of the liver: technical challenges and prospects for the future. *Magn Reson Med Sci* 2005; 175-86.
9. Le Bihan D, Breton E, Lallemand D, Grenier P, Cabanis E, Laval-Jeantet M. MR imaging of intravoxel incoherent motions: application to diffusion and perfusion in neurologic disorders. *Radiology* 1986; 401-7.
10. Kanematsu M, Goshima S, Watanabe H, Kondo H, Kawada H, Noda Y, Moriyama N. Diffusion/perfusion MR imaging of the liver: practice, challenges, and future. *Magn Reson Med Sci* 2012; 151-61.
11. Charles-Edwards EM, deSouza NM. Diffusion-weighted magnetic resonance imaging and its application to cancer. *Cancer Imaging* 2006; 135-43. Doi: 10.1102/1470-7330.2006.0021.
12. Thoeny HC, De Keyzer F. Extracranial applications of diffusion-weighted magnetic resonance imaging. *Eur Radiol* 2007; 1385-93. Doi: 10.1007/s00330-006-0547-0.
13. Nasu K, Kuroki Y, Nawano S, Kuroki S, Tsukamoto T, Yamamoto S, Motoori K, et al. Hepatic metastases: diffusion-weighted sensitivity-encoding versus SPIO-enhanced MR imaging. *Radiology* 2006; 122-30. Doi: 10.1148/radiol.2383041384.
14. Kele PG, van der Jagt EJ. Diffusion weighted imaging in the liver. *World J Gastroenterol* 2010; 1567-76.
15. Kwee TC, Takahara T, Ochiai R, Nieuvelstein RA, Luijten PR. Diffusion-weighted whole-body imaging with background body signal suppression (DWIBS): features and potential applications in oncology. *Eur Radiol* 2008; p. 1937-52. Doi: 10.1007/s00330-008-0968-z.
16. Pedro MS, Semelka RC, Braga L. MR imaging of hepatic metastases. *Magn Reson Imaging Clin N Am* 2002; 15-29.
17. Goshima S, Kanematsu M, Kondo H, Yokoyama R, Kajita K, Tsuge Y, Watanabe H, et al. Diffusion-weighted imaging of the liver: optimizing b value for the detection and characterization of benign and malignant hepatic lesions. *J Magn Reson Imaging* 2008; 691-7. Doi: 10.1002/jmri.21467.
18. Haider MA, Farhadi FA, Milot L. Hepatic perfusion imaging: concepts and application. *Magn Reson Imaging Clin N Am* 2010;465-75, x. Doi: 10.1016/j.mric.2010.07.009.
19. Outwater EK. Imaging of the liver for hepatocellular cancer. *Cancer Control* 2010; 72-82.
20. Gourtsoyianni S, Papanikolaou N, Yarmenitis S, Maris T, Karantanis A, Gourtsoyiannis N. Respiratory gated diffusion-weighted imaging of the liver: value of apparent diffusion coefficient measurements in the differentiation between most commonly encountered benign and malignant focal liver lesions. *Eur Radiol* 2008; 486-92. Doi: 10.1007/s00330-007-0798-4.
21. Koh DM, Brown G, Riddell AM, Scurr E, Collins DJ, Allen SD, Chau I, et al. Detection of colorectal hepatic metastases using MnDPDP MR imaging and diffusion-weighted imaging (DWI) alone and in combination. *Eur Radiol* 2008; 903-10. Doi: 10.1007/s00330-007-0847-z.
22. Taouli B, Koh DM. Diffusion-weighted MR imaging of the liver. *Radiology* 2010; 47-66. Doi: 10.1148/radiol.09090021.
23. Bruix J, Sherman M, Practice Guidelines Committee AASLD. Management of hepatocellular carcinoma. *Hepatology* 2005; 1208-36. Doi: 10.1002/hep.20933.
24. Heiken JP, Weyman PJ, Lee JK, Balfe DM, Picus D, Brunt EM, Flye MW. Detection of focal hepatic masses: prospective evaluation with CT, delayed CT, CT during arterial portography, and MR imaging. *Radiology* 1989; 47-51.
25. Koh DM, Scurr E, Collins D, Kanber B, Norman A, Leach MO, Husband JE. Predicting response of colorectal hepatic metastasis: value of pretreatment apparent diffusion coefficients. *AJR Am J Roentgenol* 2007;1001-8. Doi: 10.2214/AJR.06.0601.
26. Cui Y, Zhang XP, Sun YS, Tang L, Shen L. Apparent diffusion coefficient: potential imaging biomarker for prediction and early detection of response to chemotherapy in hepatic metastases. *Radiology* 2008; 894-900. Doi: 10.1148/radiol.2483071407.
27. Kandpal H, Sharma R, Madhusudhan KS, Kapoor KS. Respiratory-triggered versus breath-hold diffusion-weighted MRI of liver lesions: comparison of image quality and apparent diffusion coefficient values. *AJR Am J Roentgenol* 2009; 915-22. Doi: 10.2214/AJR.08.1260.
28. Oner AY, Celik H, Oktar SO, Tali T. Single breath-hold diffusion-weighted MRI of the liver with parallel imaging: initial experience. *Clin Radiol* 2006; 959-65. Doi: 10.1016/j.crad.2006.06.014.
29. Taouli B, Sandberg A, Stemmer A, Parikh T, Wong S, Xu J, Lee VS. Diffusion-weighted imaging of the liver: comparison of navigator triggered and breathhold acquisitions. *J Magn Reson Imaging* 2009; 561-8. Doi: 10.1002/jmri.21876.
30. Nishie A, Tajima T, Asayama Y, Ishigami K, Kakihara D, Nakayama T, Takayama Y, et al. Diagnostic performance of apparent diffusion coefficient for predicting histological grade of hepatocellular carcinoma. *Eur J Radiol* 2011; e29-33. Doi: 10.1016/j.ejrad.2010.06.019.